Hindawi Publishing Corporation
Journal of Radiotherapy
Volume 2014, Article ID 941072, 6 pages
http://dx.doi.org/10.1155/2014/941072

Research Article

^{90}Y-DOTA-CHS Microspheres for Live Radiomicrosphere Therapy: Preliminary *In Vivo* Lung Radiochemical Stability Studies

Alejandro Amor-Coarasa,[1] Andrew Milera,[2] Denny Carvajal,[3,4] Seza Gulec,[2,3,5] and Anthony J. McGoron[2,3]

[1] *Department of Radiology, Weill Cornell Medical College, New York City, NY 10028, USA*
[2] *Herbert Wertheim College of Medicine, Florida International University, Miami, FL 33174, USA*
[3] *Biomedical Engineering Department, Florida International University, Miami, FL 33174, USA*
[4] *Mount Sinai Medical Center, Miami, FL 33140, USA*
[5] *Jackson North Medical Center, Miami, FL 33169, USA*

Correspondence should be addressed to Anthony J. McGoron; mcgorona@fiu.edu

Received 12 September 2013; Accepted 25 November 2013; Published 3 February 2014

Academic Editor: Samer Ezziddin

Chitosan (CHS) is used to prepare microspheres of 31 ± 8 μm size. Surface modification with p-SCN-Bn-DOTA was performed. A maximum ^{90}Y capacity was found to be 12.1 ± 4.4 μCi/particle. The best obtained labeling yield was 87.7 ± 0.6%. More than 90% *in vitro* stability was found. Particle *in vitro* degradation half-life in PBS was found to be greater than 21 days. *In vivo* studies with ^{90}Y-DOTA-CHS showed more than 95% of the injected activity (decay corrected) in the lungs 24 hours after tail vein administration. ^{90}Y-DOTA-CHS *in vivo* label stability was superior to resin microspheres. The addition of p-SCN-Bn-DOTA served as a radioprotectant for bone marrow as the 5% ^{90}Y released, during the first 24 hours, was quickly eliminated via urine.

1. Introduction

In 2010 new cases of primary liver and intrahepatic bile duct cancer in the USA reached 24120, with 18910 deaths. New colorectal cancer cases reached 142570 with 51370 deaths, nearly half of the latter becoming metastatic liver cancer [1]. Liver cancer (primary or metastatic) accounts for nearly 10% of all cancers in the USA with incidence being even greater in eastern countries. Treatment modalities involve surgery [2], chemotherapy [3], chemoembolization [4], thermal ablation using radiofrequency or microwave probes [5, 6], and Radiomicrosphere Therapy (RMT) [7, 8]. The current RMT, also called Selective Internal Radiomicrosphere Treatment (SIRT), is indicated for patients with unresectable liver cancer, especially hepatic cell carcinoma and metastatic liver cancer [8]. RMT in combination with chemotherapy, also known as chemo-RMT, has been proposed to improve patient outcomes [9, 10]. The sphere size (≈30 μm) is 3 times larger than the smallest blood vessel diameter (≈10 μm), which assures the deposition of these particles as the arterial branches decrease in size. The narrow particle size distribution is necessary so that particles do not escape and pass into the venous circuit. Further, the microvascular density of liver tumors is 3–200 times greater than the surrounding liver parenchyma, making the tumor allocation preferential with respect to normal tissue [10].

The treatment progresses through several stages. When the patient is admitted several studies are performed including a ^{18}F-fluorodeoxy glucose or (^{18}F) FDG PET-CT scan to assess tumor viability and to evaluate lesion (cancer) extent. A biopsy is also recommended to determine the nature of the cancer. If RMT or chemo-RMT is indicated as the proper treatment option, the patient is then prepared for treatment planning. The patient is put under local anesthesia and a catheter is inserted through the patient's groin and guided towards the hepatic artery via fluoroscopic imaging.

Dyes are injected (hepatic angiogram) to identify the branches that go to the stomach and other organs. These branches are properly coil-embolized to prevent the particles from moving to these areas. The angiogram also provides valuable information about the main branches feeding the tumor or tumors which is used for the treatment planning as well [11]. ^{90}Y labeled microspheres (SirTEX or TheraSpheres) are later injected for therapy.

RMT is almost always accompanied by chemotherapy that is administered independently of the radiotherapeutic particles. Since these particles are nonbiodegradable, chemotherapy entrapment and *in situ* release are not possible. Polymeric microparticles that have high *in vivo* ^{90}Y radiochemical stability to protect bone marrow and also the capability to entrap chemotherapy drugs for simultaneous radio/chemotherapy are needed. A better design for these particles will most likely improve the safety and effectiveness of the current practice of RMT. Among the many materials available, a clear candidate for this application is Chitosan, a chitin derivative that has been extensively studied for drug entrapment/release and has very low (if any) *in vitro* and *in vivo* toxicity [12]. In this preliminary study, particles were allocated in the lungs via tail vein injection. Tail vein injection is a surgery free procedure to assess the *in vivo* stability of the ^{90}Y-DOTA-CHS labeling (compared to liver artery catheterization).

2. Materials and Methods

2.1. Particle Preparation and Surface Modification. Chitosan (CHS, Sigma-Aldrich, USA) particles were prepared using water in oil (w/o) emulsion technique. One mL of CHS solution (2.5% w/v solution in 2% v/v acetic acid) was added drop wise to a round bottom flask and stirred (Corning-Cole Palmer, USA) at 1150 rpm. The flask contained 20 mL of Toluene (Acros Organics, USA) and 100 μL of Tween 80 (surfactant, Sigma-Aldrich, USA). After 15 minutes 200 μL of glutaraldehyde (25% in water, FisherSci, USA) was added and the emulsion was stirred for another 105 min. Toluene was finally decanted and particles were washed three times with 200-proof ethanol (Sigma-Aldrich, USA) and lyophilized (Lab-Conco, USA). Size distribution and particle concentration were done using a hemocytometer (Reichert, USA). More than 100 particles were counted and measured for each distribution.

A 1 mg/mL solution of p-SCN-Bn-DOTA (Macrocyclics, USA, Figure 1) was prepared in Na_2HCO_3/NaH_2CO_3 buffer (Sigma-Aldrich, USA) with a pH 9.3-9.4. Particles were resuspended in 1 mL of the p-SCN-Bn-DOTA solution and stirred for 4, 12, 24, or 48 hours to form the DOTA-CHS particles. The reaction yield was evaluated using the p-SCN-Bn-DOTA absorption peak at 224 nm with a UV/Visible spectrophotometer (Varian/Agilent Technologies, Switzerland). All experiments were done in triplicate for all time points.

2.2. ^{90}Y Labeling and In Vitro Stability. A labeling study was performed at two different pH values: 5 and 7. The temperature influence on labeling was also studied using 25, 35, and 37°C. CHS microspheres and resin spheres (Provided by SirTEX, USA as unlabeled sulphonated poly(styrene-codivinylbenzene) microspheres, not for human use) were labeled for comparison in similar conditions. A 72-hour *in vitro* stability study using PBS buffer at pH 7 was performed to evaluate radiochemical purity (more than 50% of the total ^{90}Y dose is deposited after 72 hours). The radiolytic effect on the CHS microspheres due to the presence of ^{90}Y was studied during a 21-day degradation study.

Using stable YCl_3 (Sigma-Aldrich, USA) as carrier for the radioactive $^{90}YCl_3$ (Perkin-Elmer, USA), a radioactive indicator experiment was performed to calculate the maximum ^{90}Y capacity of the prepared microspheres. Experiments were also performed with resin spheres for comparison. For the *in vitro* work all activity measurements were made in an AtomLab 100 Dose Calibrator (Biodex, USA).

2.3. Animal Experiments. Sprague Dawley rats (200–225 grams, 2 per time point, Harlan, USA) were anesthetized with an Ohmeda Isotec 3 isoflurane vaporizer (GE Healthcare, USA) after being weighed. Once restrained in the supine position (completely anesthetized) a torso X-Ray was obtained (Belmont Acuray 071A, USA). Immediately after, 100 μL (8,000–10,000 particles) of the labeled microspheres, (^{90}Y-DOTA-CHS or ^{90}Y-Resin) with an activity ranging from 555 to 925 kBq (15 to 25 μCi), was injected through the lateral tail vein. Animals were imaged with noncollimated autoradiography (in the same unaltered supine position the X-Ray was obtained) at 10 min, 12 hours, and 24 hours after injection using a Packard Phosphorimager (Perkin Elmer, USA). After the last image was obtained, animals were euthanized (24 hours after injection). For all time point their lungs, liver, spleen, heart, kidneys, ribs, and 0.2 mL of blood and urine were collected, weighed, and measured for activity using a Cobra 5000 well counter (Packard, USA). One group of rats received free ^{90}Y and served as the control group. The obtained X-Rays and the autoradiography images were superimposed to provide anatomical and functional data.

For the collected organ measurements, an activity versus radiation count linearity test (with known activity samples) was performed on the gamma well counter. A test tube (similar to the ones used in the organs) was filled with absorbent paper soaked in water to simulate autoabsorption of the organs. Later, a known amount of ^{90}Y was deposited (ranging from 2 to 5 μCi, close to the activity range found in the organs) onto the paper and measured ($n = 3$ per activity point) in the well counter. Results were linear fitted and the correlation coefficient was found. Spectra obtained for the lowest and highest activity points were also compared.

3. Results and Discussion

3.1. Particle Preparation and Surface Modification. The size distribution obtained for CHS particles was an average of 30.7 ± 8.3 μm. After the preparation of the microspheres, the DOTA decoration reaction was performed (Figure 1).

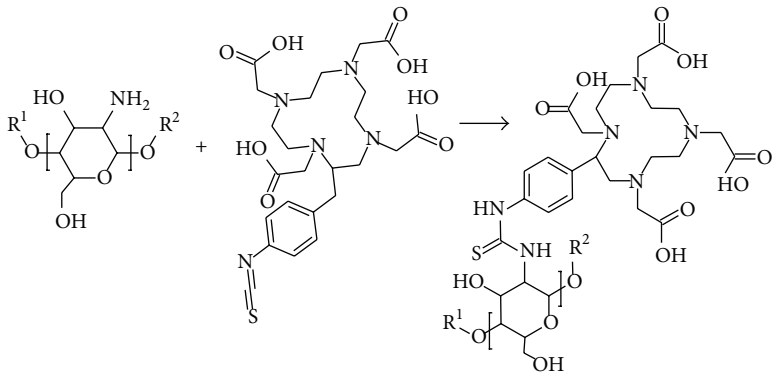

Figure 1: CHS-p-SCN-Bn-DOTA reaction.

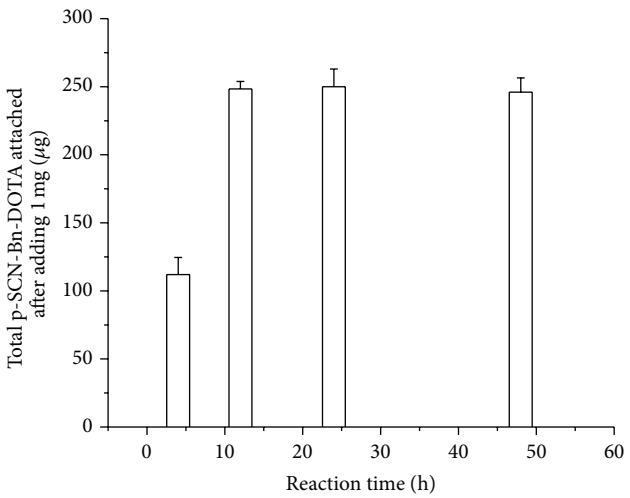

Figure 2: p-SCN-Bn-DOTA-CHS reaction kinetics. Particle surface saturation when 1 mg total p-SCN-Bn-DOTA is added to the CHS microparticles (≈100,000 in 1 mL).

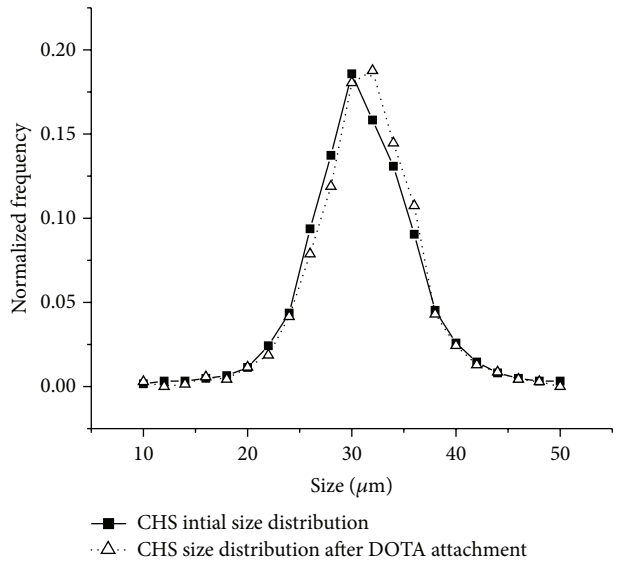

Figure 3: CHS microsphere size distribution before and after p-SCN-Bn-DOTA addition reaction.

The kinetic study for the reaction showed that saturation is reached at 12 hours (optimum reaction time), with no extra attachment of p-SCN-Bn-DOTA to CHSg after 24 or 48 hours (Figure 2). The total p-SCN-Bn-DOTA-CHS reaction yield is around 25% (with a maximum 250 μg of p-SCN-Bn-DOTA addition). The approximated 6.3 mg of CHS (total mass of 100,000 particles, 63 ng/particle) present in each preparation accounts for $2.33 \cdot 10^{19}$ available NH_2 groups in total. However, only a fraction of these groups are exposed to the microsphere surface and, to further complicate the problem, the surface is irregular.

After the p-SCN-Bn-DOTA decoration a size distribution of 31.3 ± 8.1 was obtained. The CHS microsphere distribution and morphology were not significantly changed by the p-SCN-Bn-DOTA addition reaction (Figure 3). This is expected due to the high pH (9.4) in which the reaction is being held and the already low solubility and slow degradation rate of CHS microspheres.

3.2. ^{90}Y Labeling and In Vitro Stability. Even though high labeling yields for ^{90}Y-CHS (99% yields) were previously reported by our group [13], p-SCN-Bn-DOTA was used to decorate the particle surface since the DOTA addition has the potential to increase *in vivo* stability and protect the bone marrow from ^{90}Y leaching. Maximum labeling yield for ^{90}Y-DOTA-CHS labeling was 87.7 ± 0.6%, obtained at pH = 7 and 37°C (Figure 4) after 30 minutes. Yield was dependent on both pH and temperature (Figure 4). A rise in temperature might improve the labeling; however CHS is a polysaccharide very sensitive to high temperature; thus structural damage might occur. A longer labeling time did not increase the yield. Labeling of resin spheres (Provided by SirTEX, USA as unlabeled sulphonated poly(styrene-codivinylbenzene)) showed more than 98% yield in all conditions within 10 minutes of the start of the reaction. The labeling was performed at pH = 7 only since resin spheres are typically labeled and injected in water. Yield was not dependent on temperature for the range studied.

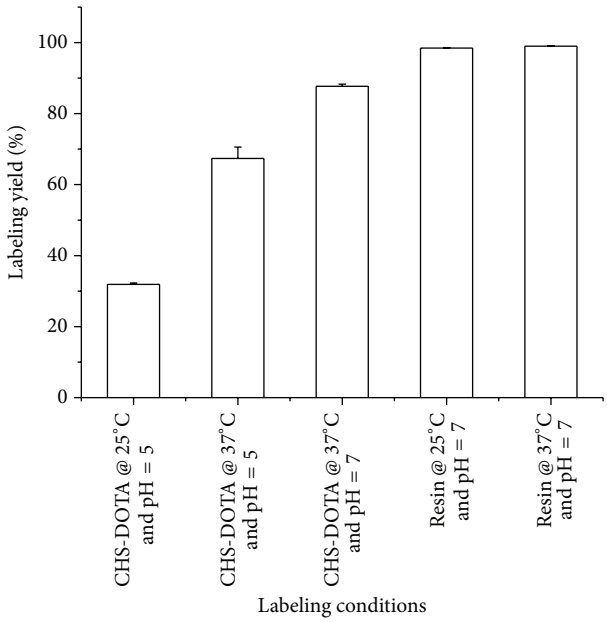

Figure 4: Labeling yields for ^{90}Y-CHS, ^{90}Y-DOTA-CHS, and ^{90}Y-Resin at different pH values and temperatures.

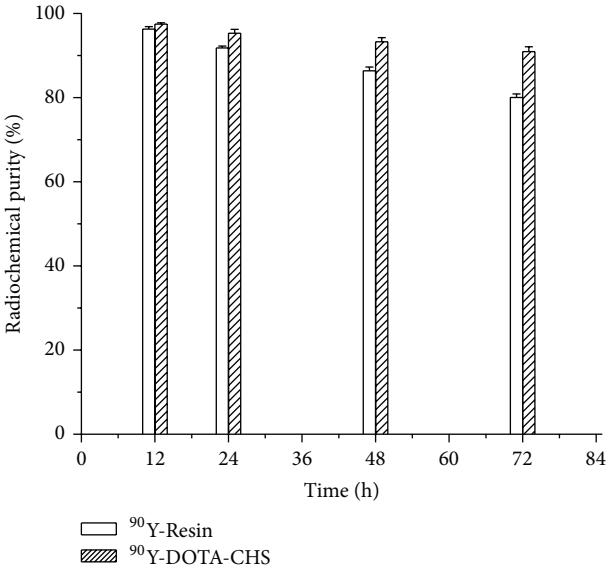

Figure 5: *In vitro* stability study for ^{90}Y-DOTA-CHS and ^{90}Y-Resin.

The *in vitro* stability was over 90% for ^{90}Y-DOTA-CHS after 72 hours compared to the 80% obtained for the resin spheres (Figure 5). Considering these positive results for ^{90}Y-DOTA-CHS, animal experiments were performed.

The extended *in vitro* degradation of the particles showed that particle integrity was maintained, although some surface degradation is seen after 21 days (Figure 6). This timeframe was chosen since more than 95% of the ^{90}Y is physically decayed by 21 days. The obtained biodegradable microspheres demonstrated a long enough half-life to adequately perform RMT while allowing for ultimate particle clearance and blood flow restoration.

Finally, the maximum labeling capacity for the CHS-p-SCN-Bn-DOTA microspheres was $12.1 \pm 4.4\ \mu$Ci/particle and for resin spheres $111.7 \pm 0.1\ \mu$Ci/particle. Hence, in a regular treatment course using $3{\cdot}10^6$ to $30{\cdot}10^6$ particles, maximum possible activity load is 36–360 Ci and 335.1–3351 Ci for CHS-p-SCN-Bn-DOTA and resin spheres, respectively. These values are 3 orders of magnitude over the regular administered dose (30–100 mCi, [10]).

3.3. Animal Experiments. Detector linearity response to activity and spectra distribution were performed as described. A high correlation coefficient ($R = 0.996$) was obtained.

The high specific gravity of the resin spheres makes particle injection difficult since they deposit fast. An injection yield (% of the total loaded to the syringe that is actually injected) of only 15% was reached (injected in water). The injection yield for the ^{90}Y-DOTA-CHS microspheres was over 50% (injected in saline solution). The initial assessment of biodistribution with a survey meter (Victoreen ASM-990, Fluke, USA) revealed a strong allocation in the lungs for the ^{90}Y-DOTA-CHS microspheres while the resin spheres distribution did not differ from the free ^{90}Y. This was interpreted to indicate that the ^{90}Y has disassociated from the resin particles as they moved through the vena cava, through the heart and into the lungs. For ^{90}Y-Resin and free ^{90}Y the 10 minutes autoradiography images showed strong ^{90}Y bone marrow and kidney allocation (Figure 7). However, organ quantification (Cobra 5000 well counter, Packard, USA) at 24 hours showed some lung allocation for ^{90}Y-Resin (Table 1).

Lung allocation of more than 95% of the injected activity (decay corrected) was detected for ^{90}Y-DOTA-CHS after 24 hours, showing a significant difference with the 23% found for the ^{90}Y-Resin. Free ^{90}Y was initially allocated in the bone marrow but only 9% remained after 24 hours. The rest of the activity was eliminated via urine. Over 4% of the injected ^{90}Y-Resin activity was found in bone marrow after 24 hours and more than 70% was eliminated by then. In contrast to this result the activity released from the lungs in the ^{90}Y-DOTA-CHS experiments resulted in only a fraction of a percent being allocated to the bone marrow, and the remaining was located in either the urine or was already eliminated.

The attachment of p-SCN-Bn-DOTA to CHS for the ^{90}Y-DOTA-CHS labeling dramatically improves the *in vivo* stability of the drug product. Furthermore the strong ^{90}Y-DOTA chelation did not release free ^{90}Y to the blood stream. The released particle degradation products (presumably as ^{90}Y-DOTA-Fragments) acted as a radioprotector of the bone marrow and other organs by being quickly eliminated to the urine.

The collected organs for the ^{90}Y-Resin and free ^{90}Y showed a very similar picture. Major damage to the kidneys was observed with low urine output and significant swelling. In the case of ^{90}Y-Resin the lungs were a bit discolored and swollen because of some radiation damage (due to the

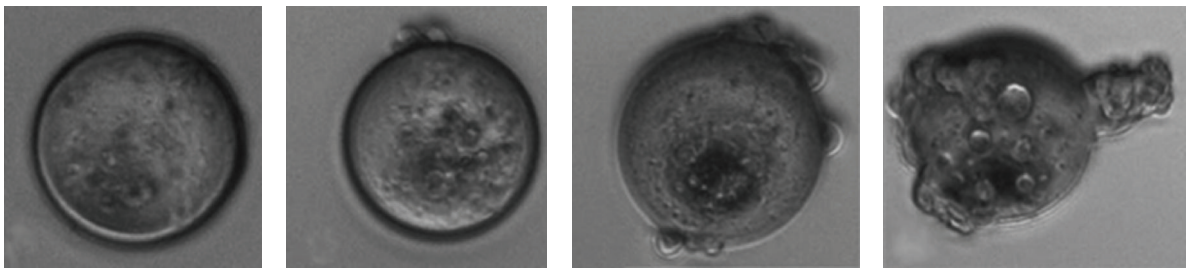

(a) (b) (c) (d)

Figure 6: Degradation of ^{90}Y-CHS microspheres after (a) 1 day, (b) 7 days, (c) 14 days, and (d) 21 days.

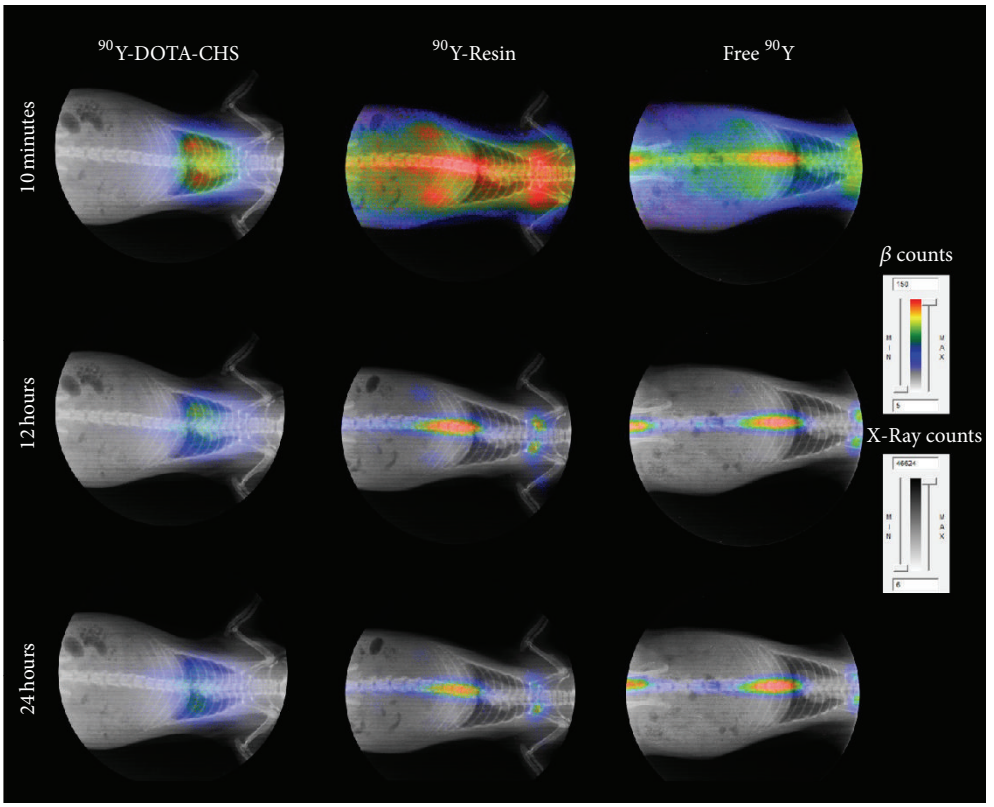

Figure 7: Non decay-corrected, un-collimated full body X-Ray/Autoradiography for ^{90}Y-DOTA-CHS, ^{90}Y-Resin and free ^{90}Y at 10 minutes, 12 and 24 hours.

allocation of 23% of the decay corrected injected activity at 24 hours). For the ^{90}Y-DOTA-CHS microspheres the radiation damage distribution was completely different. The lungs were significantly discolored and fragile after 24 hours (due to the allocation of more than 95% of the decay corrected injected activity at 24 hours) while no visible damage was seen in the kidneys and normal urine output was observed. Note that systemic venous injection of ^{90}Y microspheres so that they locate in the lungs would never be therapeutically indicated. This model was used only to investigate *in vivo* radiochemical stability and animals were not allowed to survive longer than 24 hours because of the organ damage that was expected to occur.

4. Conclusion

CHS microspheres within the 30 ± 10 μm size range were successfully obtained. Surface modification of CHS microspheres with p-SCN-Bn-DOTA was accomplished with an optimal reaction time of 12 hours. The surface decoration did not affect the original size distribution or morphology. Maximum ^{90}Y capacity was found to be 12.1 ± 4.4 μCi/particle, which means that when using $3{\cdot}10^6$ to $30{\cdot}10^6$ particles (normal therapeutic range) maximum possible activity load is 36–360 Ci (orders of magnitude higher than actual activities used). Maximum obtained labeling yield was 87.7 ± 0.6% when labeling at pH = 7 and 37°C for 30 minutes. More than 90% *in vitro* stability was found in reconstituted 1%

Table 1: Biodistribution for ^{90}Y-CHS, ^{90}Y-Resin, and free ^{90}Y at 24 hours expressed as percent of decay corrected injected dose per organ (% DC-ID/o).

Organs	Biodistribution in % DC-ID/o		
	^{90}Y-CHS	^{90}Y-Resin	Free ^{90}Y
	24 hours	24 hours	24 hours
Spleen	0.0 ± 0.0	0.1 ± 0.0	0.1 ± 0.0
Blood	0.1 ± 0.1	0.1 ± 0.1	0.1 ± 0.1
Total bone marrow	0.3 ± 0.0	4.5 ± 1.2	9.0 ± 0.4
Urine	0.9 ± 0.1	0.3 ± 0.0	0.4 ± 0.3
Right kidney	0.1 ± 0.0	0.6 ± 0.1	1.3 ± 1.0
Left kidney	0.1 ± 0.0	0.6 ± 0.1	0.7 ± 0.1
Heart	0.2 ± 0.1	0.1 ± 0.0	0.1 ± 0.0
Total lungs	95.4 ± 1.6	23.0 ± 4.3	0.2 ± 0.0
Total liver	0.3 ± 0.0	1.1 ± 0.3	1.8 ± 0.1
Eliminated	2.6 ± 1.4	69.7 ± 2.6	86.4 ± 1.3

hemoglobin lysate after 72 hours. Particle *in vitro* degradation half-life in PBS was found to be greater than 21 days. *In vivo* studies with ^{90}Y-DOTA-CHS labeled microspheres show remarkable stability with more than 95% of the injected activity (decay corrected) still in the lungs after 24 hours. ^{90}Y-DOTA-CHS performance was superior to the commercially available resin microspheres with only 23% of the injected activity (decay corrected) in the lungs after 24 hours. Autoradiography images obtained at 10 minutes showed strong release of ^{90}Y from the commercial particles. The addition of p-SCN-Bn-DOTA served to increase labeling yield and *in vivo* stability but also to act as a possible radioprotectant for other organs since less than 1% was found in bone marrow (regular ^{90}Y target organ). The 5% ^{90}Y released from the lungs during the first 24 hours was quickly eliminated via urine.

Conflict of Interests

The authors declare that there is no conflict of interests regarding the publication of this paper.

Acknowledgment

The authors acknowledge the NIH Grant no. 1 R21 CA159073-01A1 and the Rinker Family Foundation.

References

[1] A. Jemal, R. Siegel, J. Xu, and E. Ward, "Cancer statistics," *CA Cancer Journal for Clinicians*, vol. 60, no. 5, pp. 277–300, 2010.

[2] M. C. Antonetti, B. Killelea, and R. Orlando III, "Hand-assisted laparoscopic liver surgery," *Archives of Surgery*, vol. 137, no. 4, pp. 407–412, 2002.

[3] F. K. Wacker, J. Boese-Landgraf, A. Wagner, D. Albrecht, K.-J. Wolf, and F. Fobbe, "Minimally invasive catheter implantation for regional chemotherapy of the liver: a new percutaneous transsubclavian approach," *Cardiovascular and Interventional Radiology*, vol. 20, no. 2, pp. 128–132, 1997.

[4] P. Ruszniewski, P. Rougier, A. Roche et al., "Hepatic arterial chemoembolization in patients with liver metastases of endocrine tumors: a prospective Phase II study in 24 patients," *Cancer*, vol. 71, no. 8, pp. 2624–2630, 1993.

[5] K.-C. Xu, L.-Z. Niu, W.-B. He, Z.-Q. Guo, Y.-Z. Hu, and J.-S. Zuo, "Percutaneous cryoablation in combination with ethanol injection for unresectable hepatocellular carcinoma," *World Journal of Gastroenterology*, vol. 9, no. 12, pp. 2686–2689, 2003.

[6] S. A. Curley, "Radiofrequency ablation of malignant liver tumors," *Oncologist*, vol. 6, no. 1, pp. 14–23, 2001.

[7] S. A. Gulec, K. Pennington, M. Hall, and Y. Fong, "Preoperative Y-90 microsphere selective internal radiation treatment for tumor downsizing and future liver remnant recruitment: a novel approach to improving the safety of major hepatic resections," *World Journal of Surgical Oncology*, vol. 7, article 6, 2009.

[8] S. A. Gulec, G. Mesoloras, W. A. Dezarn, P. McNeillie, and A. S. Kennedy, "Safety and efficacy of Y-90 microsphere treatment in patients with primary and metastatic liver cancer: the tumor selectivity of the treatment as a function of tumor to liver flow ratio," *Journal of Translational Medicine*, vol. 5, article 15, 2007.

[9] B. Gray, G. van Hazel, M. Hope et al., "Randomised trial of SIR-Spheres plus chemotherapy versus chemotherapy alone for treating patients with liver metastases from primary large bowel cancer," *Annals of Oncology*, vol. 12, no. 12, pp. 1711–1720, 2001.

[10] S. A. Gulec and Y. Fong, "Yttrium 90 microsphere selective internal radiation treatment of hepatic colorectal metastases," *Archives of Surgery*, vol. 142, no. 7, pp. 675–682, 2007.

[11] M. Goryawala, M. R. Guillen, M. Cabrerizo et al., "A 3-D liver segmentation method with parallel computing for selective internal radiation therapy," *IEEE Transactions on Information Technology in Biomedicine*, vol. 16, no. 1, pp. 62–69, 2012.

[12] A. M. de Campos, Y. Diebold, E. L. S. Carvalho, A. Sánchez, and M. J. Alonso, "Chitosan nanoparticles as new ocular drug delivery systems: in vitro stability, in vivo fate, and cellular toxicity," *Pharmaceutical Research*, vol. 21, no. 5, pp. 803–810, 2004.

[13] A. A. Coarasa, R. Manchanda, A. McGoron, and S. Gulec, "Chitosan microspheres: therapeutic agent for liver-directed radiomicrosphere therapy," in *Proceeding of SNM*, vol. 53, 2012.